

# Familial knockin mutation of LRRK2 causes lysosomal dysfunction and accumulation of endogenous insoluble $\alpha$ -synuclein in neurons

Jason Schapansky<sup>a</sup>, Saurabh Khasnavis<sup>a</sup>, Mark P. DeAndrade<sup>a</sup>, Jonathan D. Nardozi<sup>a</sup>, Samuel R. Falkson<sup>a</sup>, Justin D. Boyd<sup>a</sup>, John B. Sanderson<sup>a</sup>, Tim Bartels<sup>a</sup>, Heather L. Melrose<sup>b</sup>, Matthew J. LaVoie<sup>a,\*</sup>

<sup>a</sup> Ann Romney Center for Neurologic Diseases, Brigham and Women's Hospital and Harvard Medical School, Boston, MA 02115, United States

<sup>b</sup> Department of Neuroscience, Mayo Clinic Jacksonville, Jacksonville, FL 32224, United States

## ARTICLE INFO

### Keywords:

LRRK2  
 $\alpha$ -Synuclein  
Tau  
Tau phosphorylation  
Lysosome  
Parkinson's disease

## ABSTRACT

Missense mutations in the multi-domain kinase LRRK2 cause late onset familial Parkinson's disease. They most commonly with classic proteinopathy in the form of Lewy bodies and Lewy neurites comprised of insoluble  $\alpha$ -synuclein, but in rare cases can also manifest tauopathy. The normal function of LRRK2 has remained elusive, as have the cellular consequences of its mutation. Data from LRRK2 null model organisms and LRRK2-inhibitor treated animals support a physiological role for LRRK2 in regulating lysosome function. Since idiopathic and LRRK2-linked PD are associated with the intraneuronal accumulation of protein aggregates, a series of critical questions emerge. First, how do pathogenic mutations that increase LRRK2 kinase activity affect lysosome biology in neurons? Second, are mutation-induced changes in lysosome function sufficient to alter the metabolism of  $\alpha$ -synuclein? Lastly, are changes caused by pathogenic mutation sensitive to reversal with LRRK2 kinase inhibitors? Here, we report that mutation of LRRK2 induces modest but significant changes in lysosomal morphology and acidification, and decreased basal autophagic flux when compared to WT neurons. These changes were associated with an accumulation of detergent-insoluble  $\alpha$ -synuclein and increased neuronal release of  $\alpha$ -synuclein and were reversed by pharmacologic inhibition of LRRK2 kinase activity. These data demonstrate a critical and disease-relevant influence of native neuronal LRRK2 kinase activity on lysosome function and  $\alpha$ -synuclein homeostasis. Furthermore, they also suggest that lysosome dysfunction, altered neuronal  $\alpha$ -synuclein metabolism, and the insidious accumulation of aggregated protein over decades may contribute to pathogenesis in this late-onset form of familial PD.

## 1. Introduction

Parkinson's disease (PD) is an aging-associated neurodegenerative disorder characterized by insoluble proteinaceous Lewy body and Lewy neurite inclusions that accumulate within multiple affected neuronal populations. The primary component of these intracellular inclusions is  $\alpha$ -synuclein ( $\alpha$ -syn), a small aggregate-prone protein that plays a central role in both idiopathic and familial forms of PD. The broad role of this small protein on the majority of PD pathogenesis makes it critical that we understand how other PD-associated genetic insults influence  $\alpha$ -syn homeostasis.

Mutations in leucine rich-repeat kinase 2 (LRRK2) are perhaps the most common genetic cause of PD, with the G2019S mutation being the most prevalent (Healy et al., 2008). Pleomorphic pathology including tauopathy or pure nigral degeneration have been reported in rare cases

(Bonifati, 2006; Zimprich et al., 2004). However, these particular monogenic forms of disease most frequently match the pathology observed in sporadic PD with both late onset and neuronal Lewy body formation. LRRK2 is a rather unique protein in that it possesses two functional domains contributing kinase and GTPase activities, as well as numerous protein-binding motifs. The current consensus in the field is that the pathogenic mutations most likely share increased kinase activity as a common gain-of-function.

LRRK2 is implicated in the regulation of Wnt signaling (Berwick and Harvey, 2012; Sancho et al., 2009), synaptic transmission (Arranz et al., 2015; Matta et al., 2012), mitochondrial function (Wang et al., 2012), and cytoskeletal polymerization (Caesar et al., 2015; Caesar et al., 2013). How these functions may contribute to the pathologic accumulation of PD-relevant proteins within neurons is unclear. Some of the earliest insights into LRRK2 neurobiology were gained from the

\* Corresponding author at: Building For Transformative Medicine Rm 10016M, 60 Fenwood Road, Boston, MA 02115, United States.

E-mail address: [mlavoie@rics.bwh.harvard.edu](mailto:mlavoie@rics.bwh.harvard.edu) (M.J. LaVoie).

overexpression of a PD-linked mutation of LRRK2 in neurons. Ectopic expression of G2019S LRRK2 was shown to increase tau phosphorylation, induce neurite retraction, and lysosome dysfunction and cell death (MacLeod et al., 2006). Further studies then confirmed the neurotoxic consequences of G2019S LRRK2 overexpression, with inhibition of LRRK2 kinase activity rescuing many of these toxic effects (Lee et al., 2010).

However, little data are currently available to explain how endogenous expression of LRRK2 containing disease-linked mutations adversely affect neuron function and whether subtle changes that long precede cell death might relate to the emergence of these more aggressive phenotypes. These questions have grown particularly more complex over the last few years, as the field has come to appreciate two observations: one, LRRK2 is only modestly expressed in neurons but highly expressed in glial and immune cell populations; and two, that dysfunction within these non-neuronal cells is likely to contribute to the pathogenesis of both LRRK2-dependent and idiopathic PD. Therefore, it is particularly important to determine whether neurons expressing endogenous LRRK2 mutation manifest phenotypes associated with known pathologic pathways involved in PD. In the present study, primary cortical cultures from recently characterized G2019S knock-in mice were analyzed. Prior work established an increase in tau phosphorylation in G2019S KI brain tissue (Yue et al., 2015), which was confirmed here and also observed in neurons cultured from these mice. Our subsequent efforts focused on lysosome biology and metabolism of  $\alpha$ -syn in G2019S neurons.

The  $\alpha$ -syn protein can be degraded by both the proteasome and the lysosome (Klucken et al., 2012; Rideout et al., 2004; Vogiatzi et al., 2008; Webb et al., 2003), suggesting that either pathway could be affected in synucleinopathies, such as PD. Our previous data demonstrated that LRRK2 knockdown results in lysosome dysfunction in myeloid cells (Schapansky et al., 2014). As neuronal  $\alpha$ -syn is a key component of disease pathology, it is crucial to determine whether expression of LRRK2 mutations at endogenous levels affect neuronal lysosome biology in a meaningful way to sufficiently alter  $\alpha$ -syn metabolism. Our data demonstrate that primary cortical neurons from homozygous G2019S KI mice had decreased lysosomal protein expression and altered morphology compared to lysosomes from WT mouse neurons. In addition, G2019S neurons had alkalinized lysosomes and decreased autophagic flux. We also examined for changes in  $\alpha$ -syn degradation and neuronal secretion, which we collectively refer to as  $\alpha$ -syn metabolism. Importantly, we observed that these lysosomal changes were associated with the accumulation of endogenous, detergent-insoluble  $\alpha$ -syn and increased neuronal  $\alpha$ -syn release. Finally, pharmacological inhibition of LRRK2 kinase activity decreased the adverse effects on  $\alpha$ -syn and rescued the lysosomal deficits exhibited by G2019S cultures. These data suggest a causal link between LRRK2 and  $\alpha$ -syn metabolism, whereby subtle lysosomal deficits induced by LRRK2 mutation may compound over decades to contribute to PD pathogenesis and Lewy body and Lewy neurite formation.

## 2. Methods and methods

### 2.1. Antibodies/reagents

The 2F12 monoclonal mouse antibody (mAb) against  $\alpha$ -syn was generated by immunizing  $\alpha$ -syn  $-/-$  (KO) mice with  $\alpha$ -syn purified from human erythrocytes as described previously (Bartels et al., 2011). Hybridoma cell lines were generated by fusion of mouse splenocytic B lymphocytes with X63-Ag8.653 myeloma cells. Antibody was generated and purified from hybridoma supernatant by Cell Essentials (Boston, MA). Syn-1 is a  $\alpha$ -syn mAb purchased from BD Biosciences (Franklin Lakes, NJ, catalog no. 610787), and used for ELISA analysis. Antibodies were purchased from as follows: LRRK2 N241A/34, Antibodies Inc./UC Davis NeuroMab; Rab5, Cell Signaling (2143S); TFR, Invitrogen (136800); p62, Abcam (56416); Actin, Sigma (A5441); LC3, MBL

(PM036); VDAC, Abcam (ab34736); LAMP1, Abcam (ab24170); LAMP2, Abcam (ab13524); Tau K9JA, DAKO, AT8 (phospho-specific tau antibody at positions S202, T205), Thermo Fisher (MN1020).

The LRRK2 inhibitor GSK2578215A (GSK) was purchased from Tocris. Cell culture media and lysosomal dyes (LysoTracker, LysoSensor) were obtained from Invitrogen. LRRK2 inhibitor CZC-25146 (CZC), chloroquine, pepstatin A, leupeptin, and DAPI were purchased from Sigma. Both LRRK2 inhibitors were used at 1  $\mu$ M, with LRRK2 kinase inhibition confirmed via blotting for phospho-S935 (UDD2, Abcam) levels in HEK293 cells transiently transfected to express LRRK2 (Fig. S1).

### 2.2. Neuronal cell culture

Heterozygous breeding pairs of mice were mated to yield WT and homozygous G2019S progeny that were then bred to obtain homozygous embryonic WT or KI pups. At day E18, cortices were dissected from male and female embryos and cells were plated in DMEM media with 10% FBS. Media was changed to Neurobasal media supplemented with B27 after 3–4 h, and mitotic inhibitors were added with a half-media change at 3 DIV to restrict glial contamination. Half-media changes were performed every three days thereafter until cells were harvested at 10 days in vitro (DIV).

### 2.3. High content analysis of lysosomal morphology

Neurons were plated 50,000 per well on 96-well imaging plates (Greiner) coated with poly-L-lysine (Sigma). At 10 DIV, neurons were labeled with LysoTracker Red (Invitrogen) according to the manufacturer's specifications, and 20 ng/ml of DAPI. Labeled live cells were imaged at 40 $\times$  magnification using the IN Cell Analyzer 2000 (GE Healthcare). Cell count, lysosome count, mean lysosome area and total lysosome area were calculated. Four fields per well were acquired using the DAPI and Cy3 channels for visualizing the DAPI and LysoTracker Red, respectively. Images were analyzed with the IN Cell Workstation software (GE Healthcare) multi target analysis protocol. Briefly, nuclei were segmented by applying a Top Hat algorithm with a minimum area of 50 square  $\mu$ m and a sensitivity level of 50 to the DAPI channel. An 8  $\mu$ m collar around the nuclei was used to distinguish the perinuclear region and the distal region of the cells (Fig. 3E, F). Lysosomes were defined as objects with a 1 to 3  $\mu$ m diameter segmented by 2 scales with a sensitivity level of 20 in the corresponding channel. Lysosomes were categorized as perinuclear or distal according to the region defined by the collar. Independent experiments were performed on WT and G2019S KI neurons plated as described above. Cells were fixed and subject to Lamp-2 immunocytochemical staining and high content image analysis.

### 2.4. LysoSensor analysis

For lysosomal pH analysis, the ratiometric dye LysoSensor Yellow/Blue (Invitrogen) was used. Cells were incubated with dye (1  $\mu$ M) for 10 min prior to rinsing 2 $\times$  with HBSS buffer. Cells were imaged using a Synergy H1 hybrid reader (Biotek; reading at excitation 329/384, emission 440/540). Calibration experiments were conducted in WT and G2019S neurons loaded with 1  $\mu$ M LysoSensor for 1 h at 37  $^{\circ}$ C, washed, and then measured for a baseline LysoSensor signal. Then, cells were incubated for 5 min at 37  $^{\circ}$ C with pH calibration standards (pH of 3.96, 4.46, 4.96, 5.47, and 5.97) prepared in 20 mM 2-(N-morpholino)ethanesulfonic acid, 110 mM KCl, and 20 mM NaCl freshly supplemented with 30  $\mu$ M nigericin and 15  $\mu$ M monensin. A pH standard curve was determined for each genotype using GraphPad Prism 7 and individual baseline pH values were interpolated from these standard curves.

## 2.5. Protein extraction/western blotting

Western blotting was performed as previously described (Schapansky et al., 2014). For protein extraction from cortices, tissue from 20 month old female mice were lysed in 1% Triton X-100 buffer (containing 50 mM HEPES, 150 mM NaCl, 1 mM EDTA, 1 mM EGTA, protease inhibitors) using 20 × strokes with a Potter-Elvehjem homogenizer. Lysates were passed through a 27 gauge needle 5 × prior to incubation on ice for 30 min. Neuronal cultures were lysed passively in 1% Triton X-100 buffer for 30 min on ice. Lysates were spun at 20,000 × g for 10 min to remove insoluble material, with the supernatant referred to as TrX soluble. For SDS-soluble proteins, the remaining pellet was extracted in 2% SDS in HEPES buffer for 60 min at room temperature followed by heating 95 °C for 10 min, then mechanically dissociated with 27 gauge needle 10 times (Triton-insoluble fraction).

## 2.6. ELISA

For  $\alpha$ -syn quantification, 96-well Multi-Array High Bind plates (MSD, Meso Scale Discovery, Rockville, MD) were used, coated with the capture antibody 2F12 diluted (6.7 ng/ $\mu$ l) and sulfo-tagged Syn1 mAb detection antibody. Following emptying of the wells, plates were blocked for 1 h at room temperature in blocking buffer (5% MSD Blocker A; TBS-T). After 3 washes with TBS-T, samples were boiled in 2% SDS before diluting 1:10 in TBS-T with 1% MSD Blocker A and 0.5% NP-40, and loaded and incubated at 4 °C overnight. Sulfo-tagged Syn1 mAb (detection Ab) was diluted in blocking buffer (6.7 ng/ $\mu$ l) and added to the plate (30  $\mu$ l volumes/well) before incubation for 1 h at room temperature, with shaking. Following 3 washes, MSD Reader buffer was added and the plates were immediately measured using a MSD Sector 2400 imager.

## 3. Results

### 3.1. G2019S LRRK2 alters lysosomal markers in vivo

Our previous work demonstrated that gene silencing or kinase inhibition of WT LRRK2 impairs autophagic capacity in myeloid cells (Schapansky et al., 2014). However, the disease-linked missense mutations in LRRK2 are thought to increase its kinase activity. The consequences of pathogenic LRRK2 mutation on lysosome function in neurons has yet to be addressed in detail. The G2019S mutation in LRRK2 is known to increase its kinase activity several-fold and this result was validated in a recently developed knock-in (KI) mouse model (Yue et al., 2015). Through DNA recombination, these animals express the mutated murine LRRK2 gene under its endogenous promoter, thus ensuring physiological LRRK2 mRNA and protein levels and distribution. Cortical tissue was homogenized from adult WT and homozygous G2019S mice, followed by protein expression analysis of several organelle marker proteins (Fig. 1A). No differences were observed between WT and G2019S animals in markers of plasma membrane (Fig. 1E; TfR), endosomal vesicles (Fig. 1F; Rab5) or mitochondria (Fig. 1G; VDAC). However, the levels of the lysosomal membrane protein LAMP1 and autophagosome protein LC3-I were both significantly decreased in adult G2019S animals compared to WT controls (Fig. 1A–C). These data were the first indication that endogenous G2019S mutation alters lysosomal biology in vivo. Furthermore, phosphorylated tau (S202) was reported to be increased in these mice (Yue et al., 2015), which was confirmed here with an independent antibody to a similar (S202/T205) phospho-tau epitope (Fig. 1I, AT8).

### 3.2. LRRK2 mutation alters lysosomal protein levels in primary cultured neurons

LRRK2 expression levels vary widely across cell types within the

brain, potentially exerting unique influences across multiple roles depending on its location. To specifically interrogate the effect of LRRK2 mutation on lysosome function in neurons, where  $\alpha$ -syn is highly expressed and accumulates in PD, primary cortical neuronal cultures from homozygous G2019S mice and WT controls were examined. Immunostaining with the neuronal marker MAP2 and the  $\alpha$ -syn antibody 2F12 demonstrated neuronal integrity and robust endogenous synuclein expression, respectively, at 10 DIV (Fig. 2A). Western blot detection revealed comparable LRRK2 protein expression in WT and G2019S cultures (Fig. 2B, C) and confirmed increased tau phosphorylation in cultured G2019S neurons, compared to WT controls (Fig. 2D–F). A further analysis of lysosomal proteins in these 10 DIV neurons revealed a significant reduction in expression of both LAMP1 and LC3-I (Fig. 2G–I), consistent with what was observed in cortical tissue homogenates (Fig. 1).

### 3.3. Endogenous G2019S LRRK2 disrupts lysosome morphology and function in neurons

The literature suggests that LRRK2 can influence lysosome morphology (Henry et al., 2015; Hockey et al., 2014; MacLeod et al., 2006). However, the impact of its endogenous mutation on lysosome function in neurons, where  $\alpha$ -syn expression is highest in the brain, has not been examined. Thus, high-content analysis of lysosome morphology was performed on WT and G2019S knockin neurons, using the live cell dye LysoTracker (Fig. 3A) with the caveat that this reagent may also identify acidic lysosome-related structures such as late endosomes and autophagosomes. Cells were co-stained with the nuclear dye DAPI to measure cell count per field and to localize nuclei and distinguish perinuclear from distal lysosomes (see description below). No significant difference was observed in cell numbers between WT and G2019S neurons, and comparable data between cultures using a live cell dye suggested that LRRK2 mutation did not affect neuronal survival (data not shown). Algorithms were generated to measure average lysosome size, number, and subcellular distribution. Results showed that G2019S neurons had decreased mean lysosome size (Fig. 3B), despite an increase in lysosomal number (Fig. 3C) and a higher total lysosomal area per cell (Fig. 3D) compared to WT neurons. Similar data were obtained following analysis of late endosomes and lysosomes via staining for LAMP-2 positive structures by immunocytochemical methods (not shown).

The G2019S mutation was shown to drive lysosomal clustering surrounding the nucleus in human fibroblasts (Hockey et al., 2014) and in follicle cells of *Drosophila* (Dodson et al., 2012). However, this was not investigated in mammalian post-mitotic neurons. Therefore, the subcellular distribution of neuronal lysosomal content was subdivided into perinuclear (within 8  $\mu$ m of the nucleus) and distal (outside the 8  $\mu$ m collar surrounding the nucleus) bins to determine if lysosomal deficits were region-specific (see schematic Fig. 3E and representative image 3F). Results showed that the G2019S mutation resulted in increased lysosome counts in both the distal and perinuclear region of the cell (Fig. 3G). Therefore, we did not find evidence of perinuclear clustering induced by endogenous G2019S in mammalian neurons. In fact, the G2019S-induced phenotypes appeared to be more pronounced in the lysosomes found distal to the nucleus.

While the kinase-augmenting G2019S mutation induced changes in lysosomal markers and organelle morphology in tissue and neurons, these data did address functional aspects of the lysosome. Lysosomal protease function is well known to be pH-dependent, requiring an acidic luminal environment for optimal activity (Appelqvist et al., 2013; Turk et al., 1995). To detect potential functional defects in G2019S neuronal lysosomes, lysosomal pH was measured using the pH-sensitive dye LysoSensor. Analysis revealed that lysosomal acidification was decreased in the G2019S neurons compared to WT controls (Fig. 3H). Further calibration of these changes with known pH standards revealed statistically significant increase in intraluminal lysosome

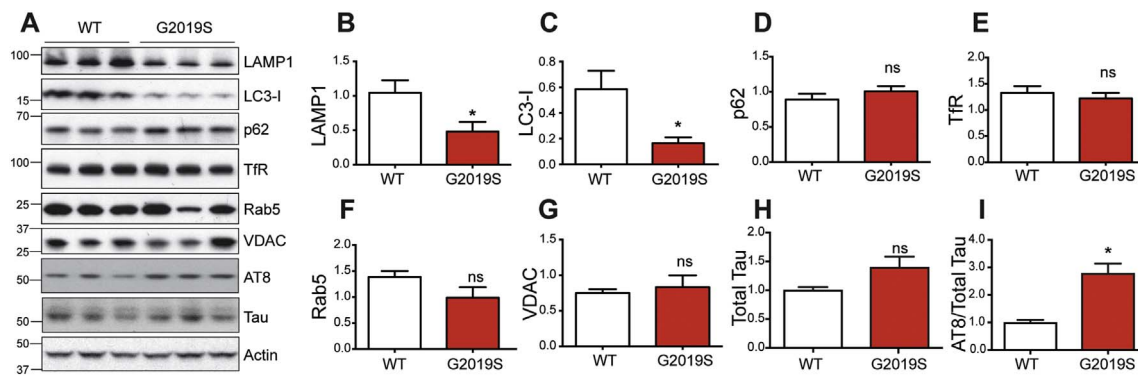


**Fig. 1. G2019S mutation of endogenous LRRK2 affects lysosomal protein markers in vivo.** Cortices from WT and homozygous KI mice at ~20 months were homogenized and immunoblotted for different organelle markers. Representative images are shown in (A), with quantification of TfR (B), LAMP1 (C), LC3-I (D), p62 (E), Rab5 (F), and VDAC (G). Quantification was performed on 5 WT and 6 KI brain samples, with all protein levels normalized to actin with the exception of phospho-tau (AT8) which was normalized to total tau (Student *t*-test,  $n = 5-6$ , \* denotes  $p < 0.05$ ).

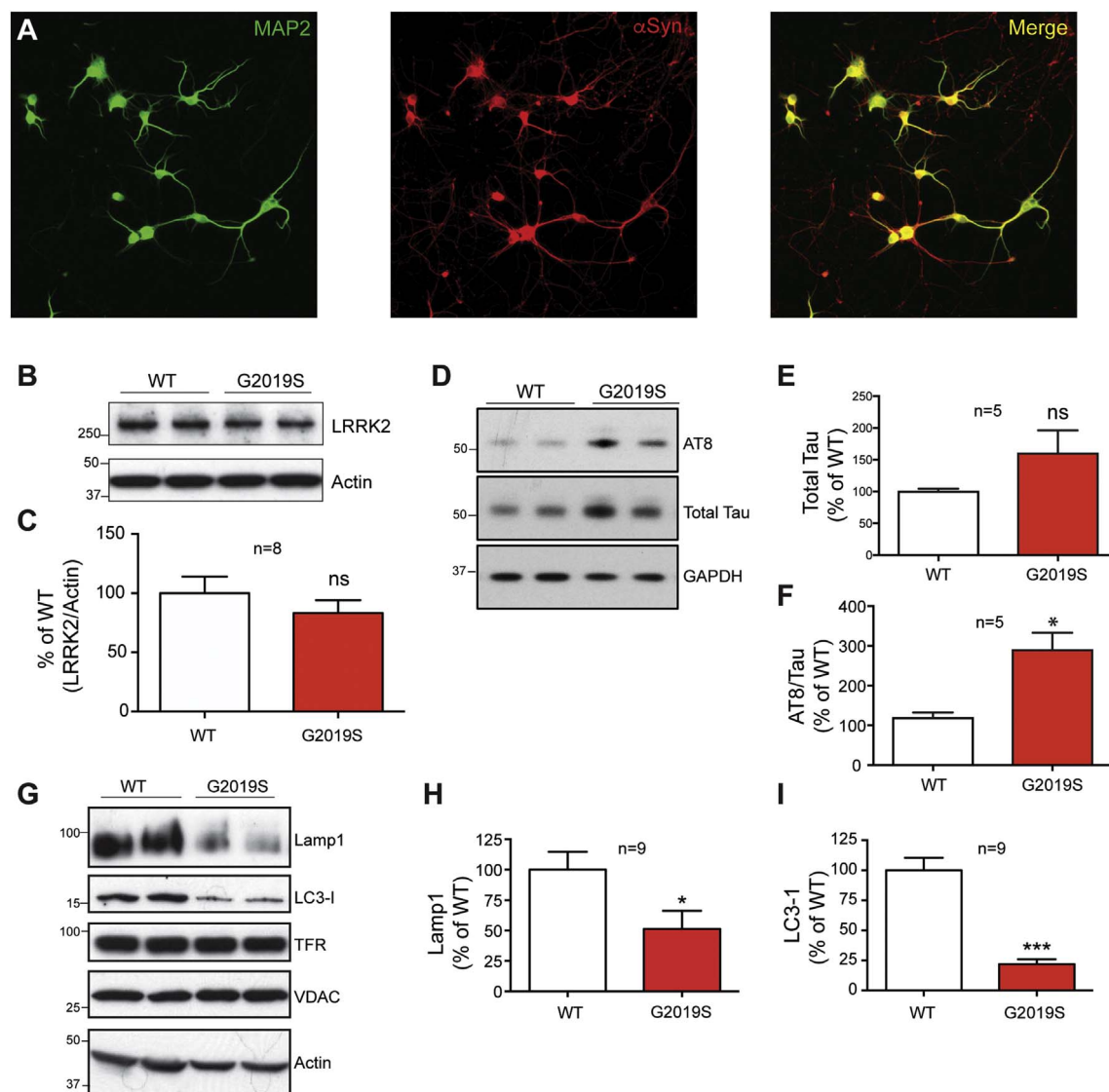


**Fig. 2. Primary cultured neurons from G2019S mice display changes in lysosomal proteins.** Cortical neurons were isolated from embryonic day 18 WT and homozygous G2019S KI mice, and cultured for 7–10 DIV. (A) Neurons at 10 DIV were immunostained with neuronal marker MAP2, and with 2F12 antibody to verify  $\alpha$ -syn expression. LRRK2 expression (B) was examined in 10 DIV WT and G2019S cortical neurons, followed by quantification against actin protein levels (C). Total and phospho-tau levels were also quantified by (D) Western blot and (E, F) densitometric analysis compared to GAPDH loading control and total tau, respectively (Student's *t*-test,  $n = 5$ , \* denotes  $p < 0.05$ ). Whole cell lysates from DIV 10 neurons were protein normalized and analyzed by Western blot for expression of LAMP1, LC3-1, TfR and VDAC (G). Levels of LAMP1 and LC3-1 were compared to actin loading control for quantification (H and I, Student *t*-test,  $n = 9$ , \* denotes  $p < 0.05$ , \*\*\* $p < 0.001$ ).



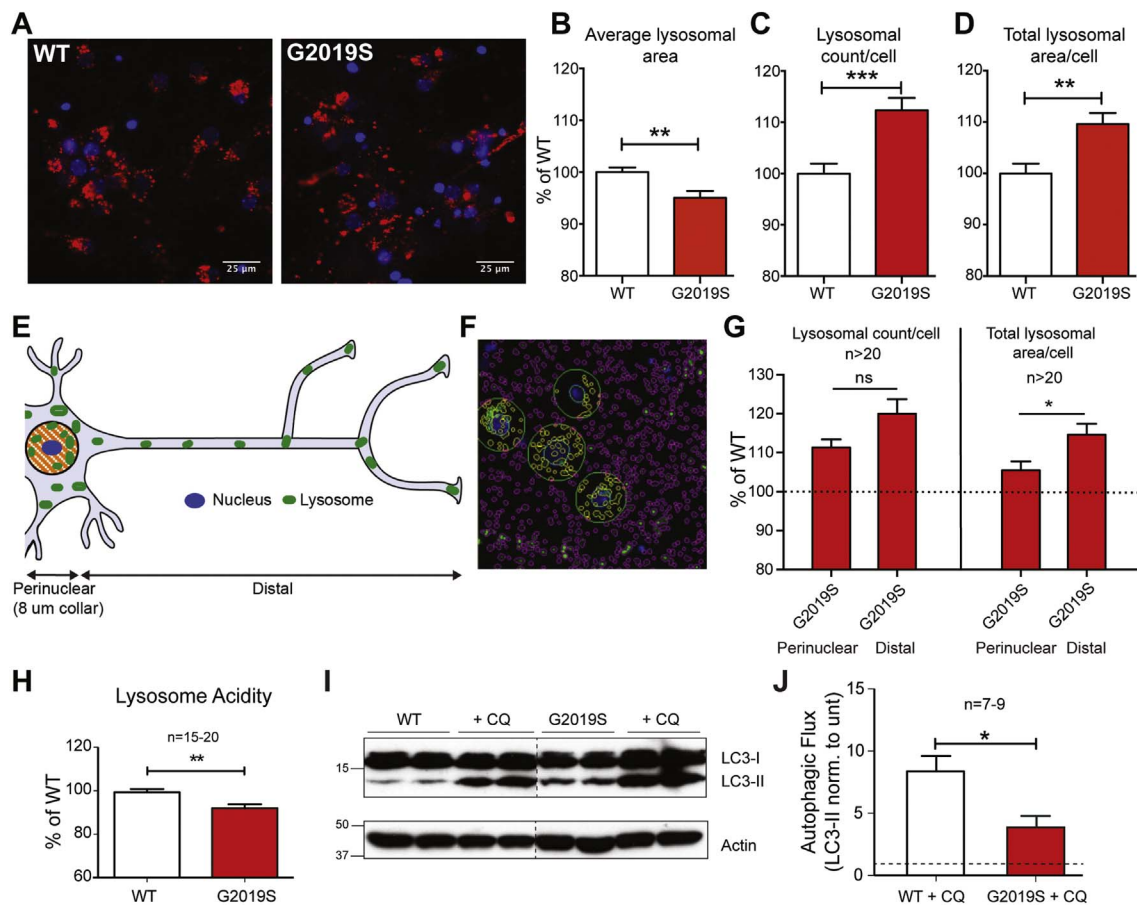


**Fig. 3. G2019S neurons have altered lysosomal morphology and function.** WT and G2019S cortical neurons were stained with LysoTracker Red dye and DAPI nuclear stain (A) and imaged on an IN Cell 2000 HCA automated imager. Lysosomal parameters including (B) average lysosomal area, (C) lysosomal count and (D) lysosomal area/cell are shown (\*\*,  $p < 0.005$ ; Student *t*-test, \*\*\*,  $p < 0.001$ ). Changes in relation to the spatial location of lysosomes (E, F) were measured in WT and G2019S neurons, split into perinuclear (within 8  $\mu$ m of nucleus; yellow) or distal (outside of 8  $\mu$ m collar, purple) categories. G2019S lysosomes in perinuclear and distal categories (G) were normalized to WT (as indicated by dotted line), prior to a direct comparison (Student *t*-test,  $n = 20$ , \* denotes  $p < 0.05$ ). All lysosomal analyses were collated from independent experiments ( $N = 5-8$ ), with a total  $n > 20$  wells/phenotype. Lysosomal acidity (H) was measured using live cell dye LysoSensor, expressed as a percentage of WT (from 5 separate experiments,  $n = 15-20$  wells/phenotype; Student *t*-test, \*\* denotes  $p < 0.005$ ). WT and G2019S cells were treated with 5  $\mu$ M chloroquine for 16 h and LC3-II levels were assessed by WB (I). For quantification of basal autophagic flux (J), the fold-increase of LC3-II/actin levels following CQ treatment over untreated cells was used (from 3 experiments,  $n = 7-9$ ; Student *t*-test, \* denotes  $p < 0.05$ ).

pH from 5.73 to 6.13 ( $p < 0.001$ ;  $n = 25$ ).

The alkalization of G2019S neurons would likely indicate decreased proteolytic processing by the neurons. To assess this, we examined neuronal autophagic flux, the rate of autophago-lysosome assembly and turnover and a component of overall protein and organelle degradation within the cell. Since lysosomes contribute the proteolytic machinery to the autophago-lysosome, and because many of proteins involved in macroautophagy are also substrates of this clearance pathway, lysosomal deficiency would reduce autophagic flux. The levels of basal and chloroquine-sensitive LC3-II protein were analyzed from both WT and G2019S knockin primary neurons, an established protocol for analyzing autophagic flux (Klionsky et al., 2016; Mizushima et al., 2010). Increased basal levels of LC3-II in untreated G2019S compared to WT cultures suggested poor lysosomal activity and decreased autophagosome turnover in G2019S neurons (Fig. 3I). However, this interpretation was conclusively validated by the chloroquine-treated samples where one can readily distinguish increased LC3-II conversion from failed LC3-II degradation. The substantially elevated LC3-II levels in WT neurons was indicative of normal basal autophagic flux in neurons. However, LC3-II levels were only slightly increased upon chloroquine treatment in G2019S neurons (Fig. 3I), demonstrating decreased autophagic flux. These data are quantified across multiple independent cultures as a ratio of LC3-II levels  $\pm$  chloroquine in Fig. 3J. These results demonstrate that G2019S knockin neurons possess deficits in lysosomal protein clearance that could be

relevant to the proteinopathy in late onset PD.

#### 3.4. Perturbation of lysosome function alters neuronal metabolism and release of endogenous $\alpha$ -syn

$\alpha$ -Syn is a highly abundant protein in neurons, and disruption of lysosomal processes can influence its metabolism (Lee et al., 2004; Li et al., 2004; Vogiatzi et al., 2008). To confirm these observations and extend these data to investigate the impact of lysosomal disturbance on the solubility of  $\alpha$ -syn, primary cortical neurons from WT mice were treated with various lysosome inhibitors and cell lysates separated into detergent-soluble and insoluble fractions. Lysosomal metabolism of  $\alpha$ -syn was initially assessed with inhibitors of lysosomal enzymes cathepsin D (pepstatin A) or cathepsin B (leupeptin), both of which have been shown to degrade  $\alpha$ -syn (Crabtree et al., 2014; Cullen et al., 2009; McGlinchey and Lee, 2015). Following treatment for 3 days, proteins were sequentially extracted with Triton X-100 (TrX) detergent followed by SDS to separate the major pool of TrX-soluble  $\alpha$ -syn from the smaller detergent-insoluble  $\alpha$ -syn. As predicted, acute lysosomal protease inhibition had no effect on the major ( $> 80\%$  of total) soluble pool of  $\alpha$ -syn (Fig. 4A) or on  $\alpha$ -syn mRNA levels (data not shown). Inhibition of cathepsin D had little effect on insoluble  $\alpha$ -syn (Fig. 4B), but cathepsin B inhibition resulted in a significant increase in detergent-insoluble  $\alpha$ -syn (Fig. 4B). To model the manner of effect observed in G2019S LRRK2 neurons,  $\alpha$ -syn levels were examined following treatment with the

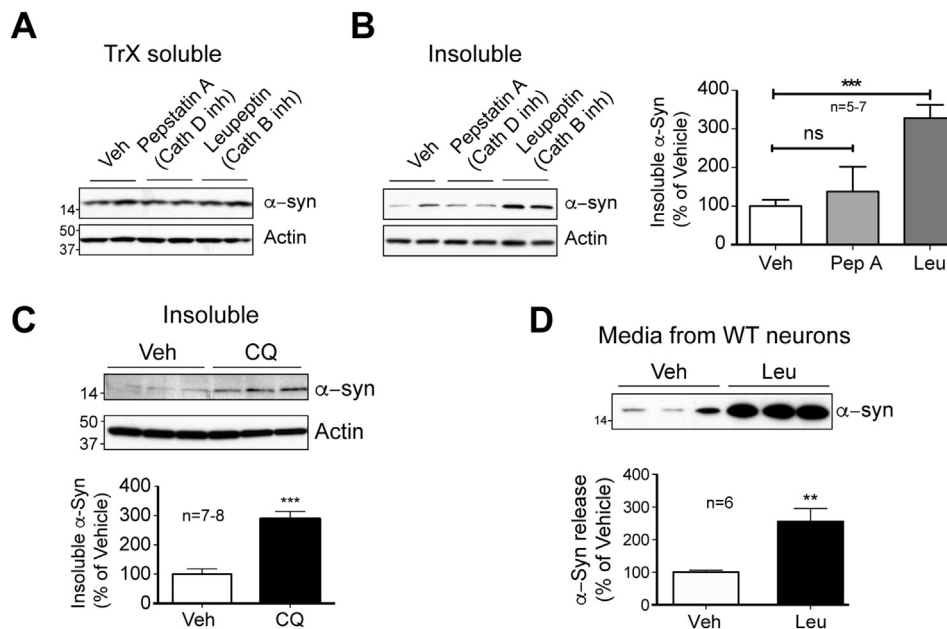


**Fig. 4. Lysosomal inhibition alters metabolism of neuronal  $\alpha$ -syn.** At 7 DIV, WT cells were treated with vehicle (1.4% MeOH), pepstatin A (10  $\mu$ g/ml), or leupeptin (10  $\mu$ g/ml), and treated again at 9 DIV. On 10 DIV, cells were scraped and extracted in TrX buffer (soluble) (A) and TrX-insoluble (B) samples were protein normalized and immunoblotted with  $\alpha$ -syn and actin antibodies. Blot quantification shown to the right is expressed as a % of the WT  $\alpha$ -syn/actin ratio (3 independent experiments,  $n = 5-7$ ; Student  $t$ -test, \*\*\* denotes  $p < 0.001$ ). (C) At 9 DIV, WT neurons were treated with 5  $\mu$ M chloroquine for 16 h, prior to extraction as previously. Quantification of SDS-soluble  $\alpha$ -syn is shown below (3 experiments,  $n = 7-8$ ; Student  $t$ -test, \*\*\* denotes  $p < 0.001$ ). (D) Following treatment with of WT neurons with either vehicle or leupeptin at 7–9 DIV, a sample of media was taken and mixed with  $2 \times$  Laemmli sample buffer, and probed for  $\alpha$ -syn by WB. To confirm Western blot quantification of the leupeptin-induced increase in secreted  $\alpha$ -syn, data from a sandwich ELISA is shown to the right (3 experiments,  $n = 6$ ; Student  $t$ -test, \*\* denotes  $p < 0.005$ ).

established lysosomal alkalinizing agent, chloroquine (Mizushima et al., 2010). Treatment with chloroquine resulted in a similar increase in insoluble  $\alpha$ -syn to those treated with leupeptin (Fig. 4C, quantified adjacent), confirming the importance of lysosomal proteases and luminal acidification to  $\alpha$ -syn metabolism in neurons.

Largely an intracellular protein,  $\alpha$ -syn is also released from neurons via an unknown mechanism (El-Agnaf et al., 2003; Emmanouilidou et al., 2010; Lee et al., 2005; Lee et al., 2011) that may be affected by cell stress and changes in autophagic flux (Alvarez-Erviti et al., 2011; Danzer et al., 2012; Hasegawa et al., 2011; Jang et al., 2010; Lee et al., 2013). To test whether lysosomal impairment increases the release of endogenous  $\alpha$ -syn from WT neurons, media was collected from neurons treated with vehicle or the cathepsin B inhibitor, leupeptin. Inhibition of cathepsin B resulted in significantly elevated  $\alpha$ -syn release, as observed by both Western blot (Fig. 4D, left) and ELISA analysis (Fig. 4D, right). These data demonstrate that inhibition of lysosomal function can severely alter  $\alpha$ -syn metabolism, increasing both accumulation of insoluble  $\alpha$ -syn and secretion of endogenous  $\alpha$ -syn by neurons.

### 3.5. Endogenous expression of G2019S LRRK2 results in the accumulation of insoluble $\alpha$ -syn and enhanced $\alpha$ -syn release

The pathogenic role of  $\alpha$ -syn in sporadic and familial PD, and the presence of classic neuronal Lewy body pathology in familial LRRK2 patients, make it especially important to examine LRRK2-dependent changes in the neuronal metabolism of this protein. Potent inhibition of lysosomal activity in WT neurons had a strong effect on  $\alpha$ -syn accumulation (Fig. 4B, C), but the impact of the PD-linked G2019S mutation in LRRK2 has not yet been examined in neurons. Therefore, total cellular proteins from G2019S and WT neurons were sequentially extracted to quantify both TrX-soluble and detergent insoluble  $\alpha$ -syn. Levels of endogenous TrX-soluble  $\alpha$ -syn were unchanged between WT and G2019S neurons (Fig. 5A). However, insoluble  $\alpha$ -syn was significantly elevated in G2019S neurons compared to WT neurons (Fig. 5B), suggesting that G2019S-containing neurons have a decreased capacity to metabolize  $\alpha$ -syn.

The discovery of extracellular  $\alpha$ -syn and its cell-to-cell transfer may provide an important clue as to how Lewy bodies arise throughout the PD brain (Desplats et al., 2009; Hansen et al., 2011; Kordower et al., 2008). Therefore, examining whether G2019S-LRRK2 might promote the release of endogenous  $\alpha$ -syn from neurons could be important step

in understanding the emergence and progression of PD pathology. To test this hypothesis, culture media from DIV 10 WT and G2019S neurons was assessed by an  $\alpha$ -syn sandwich ELISA. The levels of  $\alpha$ -syn were significantly greater from the conditioned media of G2019S neurons compared to WT controls (Fig. 5C), suggesting that LRRK2 mutation in neurons also enhanced the spread of  $\alpha$ -syn.

### 3.6. Inhibition of LRRK2 kinase activity reverses G2019S-induced lysosomal phenotypes

The G2019S mutation is the best-characterized PD-associated LRRK2 mutation, with a well-documented multi-fold increase in kinase activity (Greggio et al., 2009; Li et al., 2007; West et al., 2005; Yue et al., 2015). For this reason, numerous pharmacological inhibitors have been developed, both as tool compounds to assess the biological function of LRRK2 and as potential therapeutics. It was reasoned that a reduction in LRRK2 kinase activity should reverse G2019S-induced phenotypes, including the alterations in lysosomal morphology. To test this hypothesis, WT and G2019S neurons were treated with the LRRK2-specific inhibitor GSK2578215A (GSK) prior to lysosome morphology analysis. Some reports suggest LRRK2 kinase inhibitors can affect LRRK2 protein stability, therefore we examine acute and long-term treatment in WT and G2019S neurons. However, we observed that LRRK2 inhibitors had no effect on total levels of LRRK2 in neurons from either genotype (Fig. S1B). The GSK compound elicited minor trends for decreased lysosome number and area that were not significant in these treatment conditions. (Fig. 6A, B). However, LRRK2 inhibition in G2019S neurons resulted in greater effects that were significant, with reductions in both lysosomal number and lysosomal area per neuron to WT levels (Fig. 6A, B), effectively rescuing the G2019S phenotype under the conditions tested.

We then sought to further characterize the effects of the G2019S mutation on lysosomal acidification and determine the role of increased LRRK2 kinase activity in this effect. Thus, lysosome acidity was measured in WT, G2019S, and G2019S inhibitor-treated neurons, as described previously. GSK treatment rescued the defect in lysosome acidity in G2019S KI neurons to WT levels (Fig. 6C), consistent with the hypothesis that G2019S mediated changes in cell function occur through autonomous increases in its kinase activity.

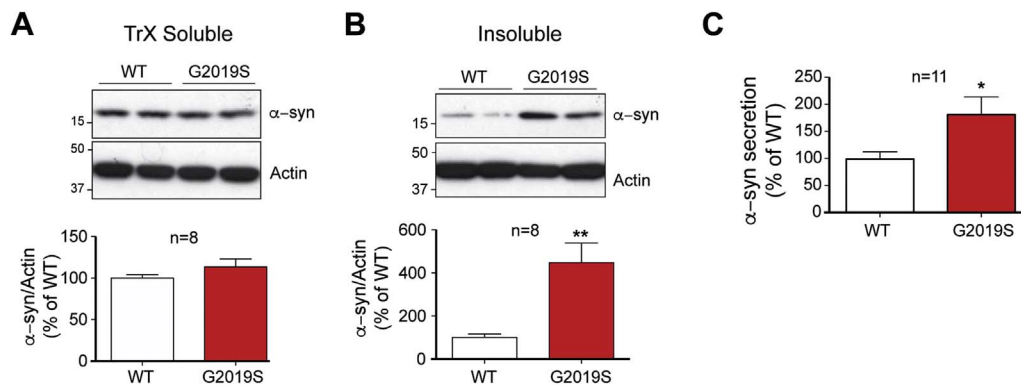


**Fig. 5.** G2019S mutation alters neuronal metabolism of endogenous  $\alpha$ -syn. WT and G2019S neurons were sequentially extracted with TrX (A) followed by SDS buffers (B), and  $\alpha$ -syn levels were analyzed by WB and quantified below (3 experiments,  $n = 8$ ; Student  $t$ -test, \*\* denotes  $p < 0.005$ ). (C) Aliquots of media taken from untreated DIV 10 G2019S and WT neuronal cultures were analyzed by ELISA for secreted  $\alpha$ -syn (4 experiments,  $n = 11$  wells; Student  $t$ -test, \* denotes  $p < 0.05$ ).

### 3.7. LRRK2 kinase inhibition rescues perturbations in $\alpha$ -syn metabolism

To determine whether this correction in lysosomal parameters results in functional improvements in lysosome biology, we probed the levels of detergent insoluble  $\alpha$ -syn. As described above, G2019S LRRK2 neurons were treated with the GSK compound for 3 DIV, prior to subcellular fractionation at DIV 10. Treatment with the GSK compound successfully decreased insoluble  $\alpha$ -syn levels (Fig. 6D), correlating well with reversal of G2019S-induced lysosomal morphology changes (Fig. 6A–C).

To further establish the correction of relevant G2019S phenotypes, we utilized a second and structurally distinct kinase inhibitor, CZC25146 (CZC). Standard practices in primary neuronal culture involve half-media changes every three days. These feedings could potentially dilute the secreted  $\alpha$ -syn pool and subsequently prevent its detection. To include an analysis of changes in neuronal release of  $\alpha$ -syn along with insoluble  $\alpha$ -syn from the sample cultures in parallel, we extended the duration of treatment with LRRK2 inhibitor to capture drug-mediated changes in media levels of  $\alpha$ -syn. Data showed that CZC significantly decreased insoluble  $\alpha$ -synuclein levels (Fig. 6E). To determine whether LRRK2 kinase inhibition would also reduce the neuronal release of  $\alpha$ -syn conditioned media from vehicle and CZC-treated G2019S neurons was probed by Western blot. Treatment with CZC significantly decreased the levels of  $\alpha$ -syn found in the media of G2019S neurons (Fig. 6F), further indicating that the effects of LRRK2 G2019S mutation on  $\alpha$ -syn is kinase-dependent.

## 4. Discussion

The PD-linked kinase LRRK2 has been broadly implicated in many facets of cell biology. It may influence development, the peripheral immune system, and synaptic release mechanisms. What is currently lacking, however, is an understanding of how LRRK2-regulated cell biologies impinge upon pathways known to contribute to PD etiology. LRRK2-PD is most commonly associated with intraneuronal accumulation of the  $\alpha$ -syn protein into Lewy bodies and Lewy neurites but can present with tauopathy or pure nigral degeneration. Therefore, proteostasis and the clearance mechanisms of misfolded proteins, and in particular  $\alpha$ -syn, have moved to the forefront of proposed models of PD.

The evaluation of LRRK2 null systems and the consequences of LRRK2 kinase inhibition have demonstrated a critical role for LRRK2 in lysosome biology (Baptista et al., 2013; Fuji et al., 2015; Herzig et al., 2011; Tong et al., 2010). However, much of these data were collected from analysis of peripheral tissue. From this important work emerge two crucial unanswered questions: 1) How does PD-linked mutation of LRRK2 affect lysosome function in neurons? 2) Do LRRK2-induced lysosome disturbances affect  $\alpha$ -syn proteostasis? Therefore, we sought to examine whether the most common LRRK2 mutation affects the lysosome system in neurons and whether any resultant defects would be sufficient to alter endogenous  $\alpha$ -syn turnover. A recently characterized

LRRK2-G2019S knock-in mouse model provides the ideal opportunity to study the influence of endogenous G2019S LRRK2 on lysosome function and  $\alpha$ -syn turnover in neurons. This mouse was previously shown to exhibit mild motor deficits and changes in dopamine neurochemistry (Yue et al., 2015). Furthermore, increased tau phosphorylation was reported, which we validated here.

The goal of the present study was to understand the impact of pathogenic mutation of LRRK2 mutation on lysosomal biology. The data presented here demonstrate that G2019S-LRRK2 significantly impacts the morphology and function of lysosomes and potentially other acidic organelles in primary cultured neurons, decreasing both organelle size and acidification. In addition to these defects, we found that homozygous G2019S neurons accumulate intracellular insoluble  $\alpha$ -syn and secrete more  $\alpha$ -syn into culture media, consequences that can be recapitulated in WT neurons by direct lysosome inhibition. It should be noted that preliminary experiments using a small cohort of young WT and G2019S KI mice did not reveal significant changes in tissue  $\alpha$ -syn levels. However, formal investigation particularly in aged animals is warranted. Finally, pharmacological inhibition of G2019S LRRK2 restores both lysosomal morphology and acidification, and reverses the adverse effects on  $\alpha$ -syn proteostasis. These data suggest a cell-autonomous mechanism by which PD-associated mutations in LRRK2 alter  $\alpha$ -syn homeostasis in cultured neurons, in part through lysosomal dysfunction.

Increased production of WT  $\alpha$ -syn, independent of its aggregation-prone mutation, is sufficient to cause disease (Chartier-Harlin et al., 2004; Ibanez et al., 2004; Ross et al., 2008). Therefore, decreased clearance of  $\alpha$ -syn could likewise play an important role in the etiology of PD. The pathways regulating  $\alpha$ -syn metabolism deserve formal investigation. Inhibiting autophagy in cell lines overexpressing  $\alpha$ -syn results in an accumulation of the protein, supporting the physiological importance of lysosomes to  $\alpha$ -syn turnover (Lee et al., 2013; Poehler et al., 2014). In our hands inhibition of cathepsin B-like activity, but not cathepsin D-like protease activity, resulted in the accumulation of endogenous, insoluble  $\alpha$ -syn in WT neurons (Fig. 4B). Supporting this data is the fact that lysosomal enzymes have decreased efficiency under alkaline conditions (Appelqvist et al., 2013; Turk et al., 1995), and treatment of WT neurons with chloroquine to reduce lysosomal acidity also elevated detergent-insoluble  $\alpha$ -syn (Fig. 4C). Therefore, either a direct inhibition of lysosomal enzymes or a more general alteration in the luminal lysosome environment is sufficient to increase insoluble endogenous  $\alpha$ -syn, confirming the importance of functional lysosomes to  $\alpha$ -syn degradation in neurons. As the lysosomal proteases are pH-dependent and G2019S neurons showed a defect in lysosome acidification, it is likely that the enzymes responsible for  $\alpha$ -syn turnover are affected in these neurons.

LRRK2 has previously been shown to affect lysosome morphology, with the G2019S mutation having a strong effect. Overexpression of mutant LRRK2 in neurons or neural cell lines (MacLeod et al., 2006; Plowey et al., 2008), and astrocytes (Henry et al., 2015) results in



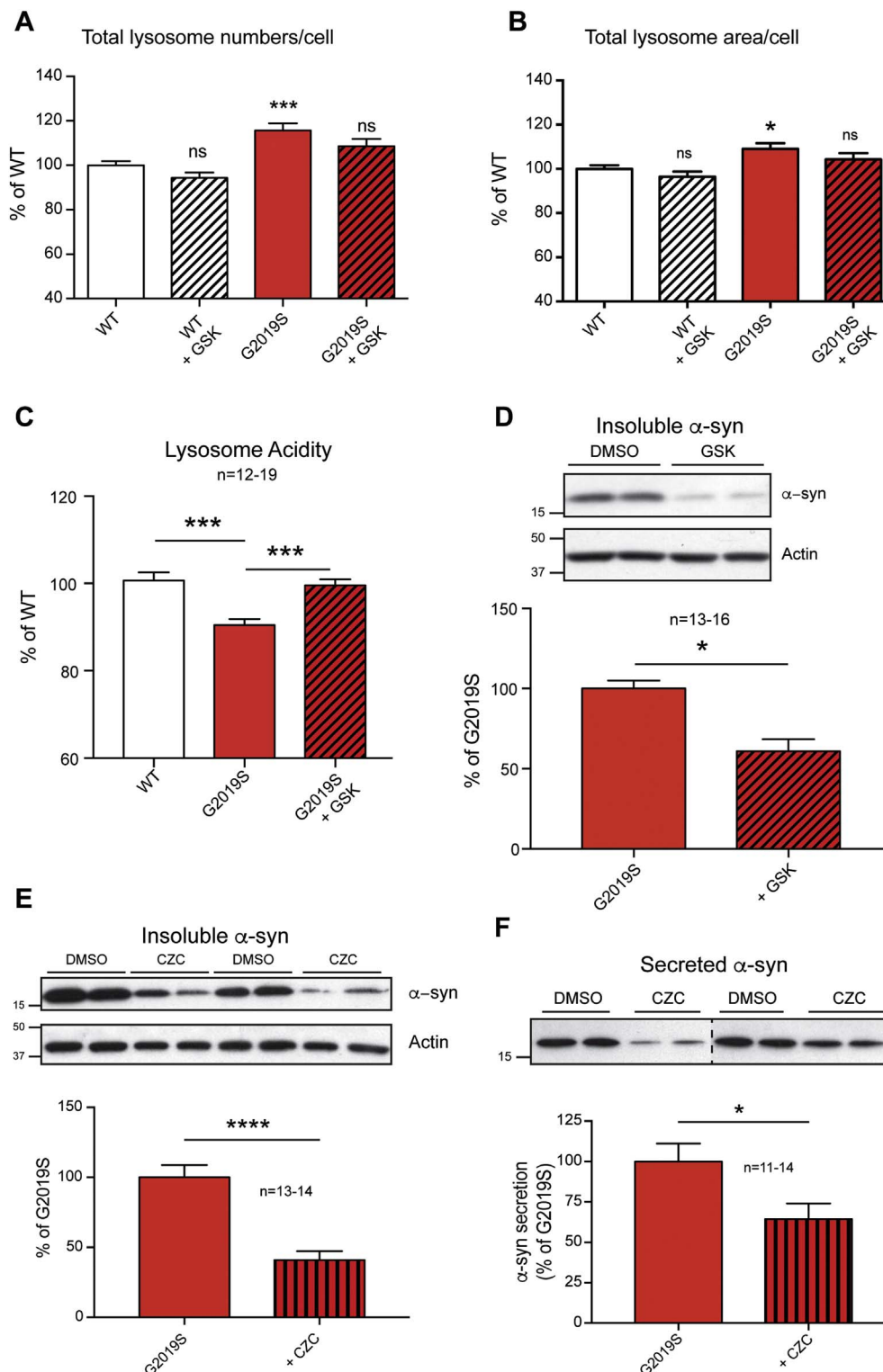


**Fig. 6. LRRK2 kinase inhibition corrects both the lysosomal defects and  $\alpha$ -syn related changes in G2019S neurons.** WT and G2019S neurons were treated with GSK LRRK2 inhibitor (1  $\mu$ M) at 7 DIV and 9 DIV, and lysosomal numbers/cell (A) and lysosomal area/cell (B) were measured (8 experiments,  $n = 24$ –33 wells; 1-way ANOVA, Dunnett's post-hoc test, \* denotes  $p < 0.05$ ). WT and G2019S neurons were treated with GSK at 7 DIV and scraped at 10 DIV. Lysosomal acidification (C) was measured after 3 DIV inhibitor treatment, and expressed as a percentage of WT (5 independent experiments,  $n = 12$ –19; One-way ANOVA with Tukey's post-hoc, \*\*\* denotes  $p < 0.001$ ). Insoluble  $\alpha$ -syn (D) was detected as previously described following 3DIV treatment with GSK (3 independent experiments,  $n = 13$ –16; One-way ANOVA with Tukey's post-hoc, \* denotes  $p < 0.05$ ). G2019S neurons were treated with CZC (1  $\mu$ M) for 7 DIV. Representative WB images of insoluble  $\alpha$ -syn and actin (E) are shown with quantification below (4 experiments,  $n = 13$ –14; Student  $t$ -test, \*\*\* denotes  $p < 0.001$ ). Culture media from the same experiments was mixed with sample buffer and (F) blotted for  $\alpha$ -syn. Densitometry of bands was normalized to total cellular protein from the corresponding sample. Representative blots are shown, with quantification of all samples below (3 independent experiments,  $n = 11$ –14; Student  $t$ -test, \* denotes  $p < 0.05$ ).

increased lysosomal size, and human fibroblasts from G2019S patients also have enlarged lysosomes (Hockey et al., 2014). However, two critical features were not yet considered. First is the analysis of differentiated neurons, and the second is a focus on matched and endogenous expression of WT and mutant LRRK2. Our results confirm a prominent effect of LRRK2 mutation on lysosomes within neurons. However, we found that neurons with endogenous G2019S LRRK2 may actually have a slightly smaller lysosomal size (Fig. 3B). In contrast, the altered lysosome acidity we observed is likely to have a greater relevance to

disease through its more direct impact on protein degradation. This deficiency in proteolysis could result in an effort by the cell to upregulate lysosome biogenesis as a compensatory mechanism, which may explain the increased lysosomal area/cell and lysosome numbers that we observed, or changes in ATP13A2, for example, observed elsewhere (Henry et al., 2015). These changes may also provide mechanistic insight into LRRK2-dependent changes in chaperone-mediated autophagy (CMA) (Orenstein et al., 2013) and mitochondrial turnover (Hsieh et al., 2016) reported by others. However, additional work will be



required to investigate potential compensatory changes in lysosome biogenesis or maturation, and their further consequences as a product of LRRK2-mediated dysfunction in neurons.

Reductions in LRRK2 expression and inhibition of LRRK2 kinase activity both decrease lysosome function and increase the accumulation of autophagic substrates in vivo and in vitro (Gomez-Suaga et al., 2012; Hinkle et al., 2012; Schapansky et al., 2014; Tong et al., 2010). One supposition drawn from these observations is that there is a linear relationship between lysosomal function and LRRK2 kinase activity and predict that mutations known to increase LRRK2 kinase activity, such as G2019S, would increase autophagic flux. Indeed, overexpression of G2019S LRRK2 has been suggested to increase autophagic activity in some systems (Cherra et al., 2013; Plowey et al., 2008; Su and Qi, 2013). However, the present study is the first to analyze autophagic flux under endogenous expression of neuronal G2019S LRRK2. Here, we report defects in lysosome function and the accumulation of detergent-insoluble  $\alpha$ -syn in G2019S KI neurons, as compared to WT controls (Figs. 3, 5). These data suggest that either loss of LRRK2 activity through genetic deletion or kinase inhibition or its augmentation due to mutation can result in similar lysosomal disturbances. It will be critical to address these issues in future studies.

Protein degradation pathways are of growing mechanistic and therapeutic interest in the study of several neurodegenerative diseases. Many genes associated with familial PD converge on either vesicle trafficking towards the lysosome, or directly or indirectly on endosome/lysosome function. Mutations in VPS35, a component of the retromer complex involved in endosome shuttling, are associated with familial PD (Vilarino-Guell et al., 2011; Zimprich et al., 2011), and can result in lysosome dysfunction in *Drosophila* (Miura et al., 2014). Rab7L1, a protein implicated in late endosomal trafficking and lysosomal maturation, is a putative binding partner of LRRK2 and may be linked to familial PD (Beilina et al., 2014; Kuwahara et al., 2016; MacLeod et al., 2013). The lysosome-resident proteins glucocerebrosidase and ATP13A2 are both extremely important in normal lysosomal function, and likewise associated with familial PD (Di Fonzo et al., 2007; Neumann et al., 2009; Park et al., 2011; Sidransky and Lopez, 2012). Lastly,  $\alpha$ -syn inhibits a specialized form of autophagy and can block its own degradation (Cuervo et al., 2004). Taken together, many proteins linked to familial PD cause lysosome dysfunction when mutated. Consistent with the hypothesis that a subset of PD-affected genes may influence  $\alpha$ -syn metabolism, the present data may provide mechanistic insight into the observation that G2019S-LRRK2 neurons display increased vulnerability to both ectopic and exogenous  $\alpha$ -syn (Daher et al., 2015; Volpicelli-Daley et al., 2016).

Familial PD caused by the G2019S LRRK2 mutation is most often associated with proteinopathy that can present with classic Lewy bodies and neurites. Unlike other familial PD variants it is not only late-onset but also weakly penetrant (Latourelle et al., 2008; Paisan-Ruiz et al., 2005; Trinh et al., 2014). Therefore, perhaps subtle G2019S phenotypes should be given greater attention. Modest lysosomal alterations and mild accumulation of insoluble  $\alpha$ -syn levels, as we have observed, could eventually compound over decades to contribute to Lewy body formation or other proteinopathy such as the tau accumulation reported in some LRRK2 cases, ultimately initiating disease pathogenesis in the human brain. Each of the G2019S phenotypes we observed here were rescued with LRRK2 kinase inhibitors. It is not at this time known how widely applicable LRRK2 inhibition would be for other familial forms of PD or idiopathic disease. Future studies must broadly evaluate the status of LRRK2 signaling in these other contexts, with the ultimate goal of determining whether increased LRRK2 signaling is a universal or even common feature of PD.

Supplementary data to this article can be found online at <https://doi.org/10.1016/j.nbd.2017.12.005>.

## Conflict of interest

None.

## Acknowledgements

The authors thank DM Walsh and Z Chen for reagents and discussion. This work was supported by the Michael J. Fox Foundation and NIH Grant NS087449 (MJL).

## References

- Alvarez-Erviti, L., et al., 2011. Lysosomal dysfunction increases exosome-mediated alpha-synuclein release and transmission. *Neurobiol. Dis.* 42, 360–367.
- Appelqvist, H., et al., 2013. The lysosome: from waste bag to potential therapeutic target. *J. Mol. Cell Biol.* 5, 214–226.
- Arranz, A.M., et al., 2015. LRRK2 functions in synaptic vesicle endocytosis through a kinase-dependent mechanism. *J. Cell Sci.* 128, 541–552.
- Baptista, M.A.S., et al., 2013. Loss of leucine-rich repeat kinase 2 (LRRK2) in rats leads to progressive abnormal phenotypes in peripheral organs. *PLoS One* 8, e80705.
- Bartels, T., et al., 2011. alpha-Synuclein occurs physiologically as a helically folded tetramer that resists aggregation. *Nature* 477, 107–110.
- Beilina, A., et al., 2014. Unbiased screen for interactors of leucine-rich repeat kinase 2 supports a common pathway for sporadic and familial Parkinson disease. *Proc. Natl. Acad. Sci. U. S. A.* 111, 2626–2631.
- Berwick, D.C., Harvey, K., 2012. LRRK2 functions as a Wnt signaling scaffold, bridging cytosolic proteins and membrane-localized LRP6. *Hum. Mol. Genet.* 21, 4966–4979.
- Bonifati, V., 2006. The pleomorphic pathology of inherited Parkinson's disease: lessons from LRRK2. *Curr. Neurol. Neurosci. Rep.* 6, 355–357.
- Caesar, M., et al., 2013. Leucine-rich repeat kinase 2 functionally interacts with microtubules and kinase-dependently modulates cell migration. *Neurobiol. Dis.* 54, 280–288.
- Caesar, M., et al., 2015. Changes in actin dynamics and F-actin structure both in synaptoneurosome of LRRK2(R1441G) mutant mice and in primary human fibroblasts of LRRK2(G2019S) mutation carriers. *Neuroscience* 284, 311–324.
- Chartier-Harlin, M.C., et al., 2004. Alpha-synuclein locus duplication as a cause of familial Parkinson's disease. *Lancet* 364, 1167–1169.
- Cherra 3rd, S.J., et al., 2013. Mutant LRRK2 elicits calcium imbalance and depletion of dendritic mitochondria in neurons. *Am. J. Pathol.* 182, 474–484.
- Crabtree, D., et al., 2014. Over-expression of an inactive mutant cathepsin D increases endogenous alpha-synuclein and cathepsin B activity in SH-SY5Y cells. *J. Neurochem.* 128, 950–961.
- Cuervo, A.M., et al., 2004. Impaired degradation of mutant alpha-synuclein by chaperone-mediated autophagy. *Science* 305, 1292–1295.
- Cullen, V., et al., 2009. Cathepsin D expression level affects alpha-synuclein processing, aggregation, and toxicity in vivo. *Mol. Brain* 2, 5.
- Daher, J.P., et al., 2015. Leucine-rich repeat kinase 2 (LRRK2) pharmacological inhibition abates alpha-synuclein gene-induced neurodegeneration. *J. Biol. Chem.* 290, 19433–19444.
- Danzer, K.M., et al., 2012. Exosomal cell-to-cell transmission of alpha synuclein oligomers. *Mol. Neurodegener.* 7, 42.
- Desplats, P., et al., 2009. Inclusion formation and neuronal cell death through neuron-to-neuron transmission of alpha-synuclein. *Proc. Natl. Acad. Sci. U. S. A.* 106, 13010–13015.
- Di Fonzo, A., et al., 2007. ATP13A2 missense mutations in juvenile parkinsonism and young onset Parkinson disease. *Neurology* 68, 1557–1562.
- Dodson, M.W., et al., 2012. Roles of the *Drosophila* LRRK2 homolog in Rab7-dependent lysosomal positioning. *Hum. Mol. Genet.* 21, 1350–1363.
- El-Agnaf, O.M., et al., 2003. Alpha-synuclein implicated in Parkinson's disease is present in extracellular biological fluids, including human plasma. *FASEB J.* 17, 1945–1947.
- Emmanouilidou, E., et al., 2010. Cell-produced alpha-synuclein is secreted in a calcium-dependent manner by exosomes and impacts neuronal survival. *J. Neurosci.* 30, 6838–6851.
- Fuji, R.N., et al., 2015. Effect of selective LRRK2 kinase inhibition on nonhuman primate lung. *Sci. Transl. Med.* 7 (273ra15).
- Gomez-Suaga, P., et al., 2012. Leucine-rich repeat kinase 2 regulates autophagy through a calcium-dependent pathway involving NAADP. *Hum. Mol. Genet.* 21, 511–525.
- Greggio, E., et al., 2009. The Parkinson's disease kinase LRRK2 autophosphorylates its GTPase domain at multiple sites. *Biochem. Biophys. Res. Commun.* 389, 449–454.
- Hansen, C., et al., 2011. alpha-Synuclein propagates from mouse brain to grafted dopaminergic neurons and seeds aggregation in cultured human cells. *J. Clin. Invest.* 121, 715–725.
- Hasegawa, T., et al., 2011. The AAA-ATPase VPS4 regulates extracellular secretion and lysosomal targeting of alpha-synuclein. *PLoS One* 6, e29460.
- Healy, D.G., et al., 2008. Phenotype, genotype, and worldwide genetic penetrance of LRRK2-associated Parkinson's disease: a case-control study. *Lancet Neurol.* 7, 583–590.
- Henry, A.G., et al., 2015. Pathogenic LRRK2 mutations, through increased kinase activity, produce enlarged lysosomes with reduced degradative capacity and increase ATP13A2 expression. *Hum. Mol. Genet.* 24, 6013–6028.
- Herzig, M.C., et al., 2011. LRRK2 protein levels are determined by kinase function and are crucial for kidney and lung homeostasis in mice. *Hum. Mol. Genet.* 20, 4209–4223.

- Hinkle, K.M., et al., 2012. LRRK2 knockout mice have an intact dopaminergic system but display alterations in exploratory and motor co-ordination behaviors. *Mol. Neurodegener.* 7, 25.
- Hockey, L.N., et al., 2014. Dysregulation of lysosomal morphology by pathogenic LRRK2 is corrected by two-pore channel 2 inhibition. *J. Cell Sci.* 128 (2), 232–238.
- Hsieh, C.H., et al., 2016. Functional impairment in Miro degradation and mitophagy is a shared feature in familial and sporadic Parkinson's disease. *Cell Stem Cell* 19, 709–724.
- Ibanez, P., et al., 2004. Causal relation between alpha-synuclein gene duplication and familial Parkinson's disease. *Lancet* 364, 1169–1171.
- Jang, A., et al., 2010. Non-classical exocytosis of alpha-synuclein is sensitive to folding states and promoted under stress conditions. *J. Neurochem.* 113, 1263–1274.
- Klionsky, D.J., et al., 2016. Guidelines for the use and interpretation of assays for monitoring autophagy (3rd edition). *Autophagy* 12, 1–222.
- Klucken, J., et al., 2012. Alpha-synuclein aggregation involves a bafilomycin A 1-sensitive autophagy pathway. *Autophagy* 8, 754–766.
- Kordower, J.H., et al., 2008. Lewy body-like pathology in long-term embryonic nigral transplants in Parkinson's disease. *Nat. Med.* 14, 504–506.
- Kuwahara, T., et al., 2016. LRRK2 and RAB7L1 coordinately regulate axonal morphology and lysosome integrity in diverse cellular contexts. *Sci. Rep.* 6, 29945.
- Latourelle, J.C., et al., 2008. The Gly2019Ser mutation in LRRK2 is not fully penetrant in familial Parkinson's disease: the GenePD study. *BMC Med.* 6, 32.
- Lee, H.-J., et al., 2004. Clearance of alpha-synuclein oligomeric intermediates via the lysosomal degradation pathway. *J. Neurosci.* 24, 1888–1896.
- Lee, H.-J., et al., 2005. Intravesicular localization and exocytosis of alpha-synuclein and its aggregates. *J. Neurosci.* 25, 6016–6024.
- Lee, B.D., et al., 2010. Inhibitors of leucine-rich repeat kinase-2 protect against models of Parkinson's disease. *Nat. Med.* 16, 998–1000.
- Lee, H.J., et al., 2011. Dopamine promotes formation and secretion of non-fibrillar alpha-synuclein oligomers. *Exp. Mol. Med.* 43, 216–222.
- Lee, H.J., et al., 2013. Autophagic failure promotes the exocytosis and intercellular transfer of alpha-synuclein. *Exp. Mol. Med.* 45, e22.
- Li, W., et al., 2004. Stabilization of alpha-synuclein protein with aging and familial Parkinson's disease-linked A53T mutation. *J. Neurosci.* 24, 7400–7409.
- Li, X., et al., 2007. Leucine-rich repeat kinase 2 (LRRK2)/PARK8 possesses GTPase activity that is altered in familial Parkinson's disease R1441C/G mutants. *J. Neurochem.* 103, 238–247.
- MacLeod, D., et al., 2006. The familial Parkinsonism gene LRRK2 regulates neurite process morphology. *Neuron* 52, 587–593.
- MacLeod, D.A., et al., 2013. RAB7L1 interacts with LRRK2 to modify intraneuronal protein sorting and Parkinson's disease risk. *Neuron* 77, 425–439.
- Matta, S., et al., 2012. LRRK2 controls an EndoA phosphorylation cycle in synaptic endocytosis. *Neuron* 75, 1008–1021.
- McGlinchey, R.P., Lee, J.C., 2015. Cysteine cathepsins are essential in lysosomal degradation of alpha-synuclein. *Proc. Natl. Acad. Sci. U. S. A.* 112, 9322–9327.
- Miura, E., et al., 2014. VPS35 dysfunction impairs lysosomal degradation of alpha-synuclein and exacerbates neurotoxicity in a *Drosophila* model of Parkinson's disease. *Neurobiol. Dis.* 71, 1–13.
- Mizushima, N., et al., 2010. Methods in mammalian autophagy research. *Cell* 140, 313–326.
- Neumann, J., et al., 2009. Glucocerebrosidase mutations in clinical and pathologically proven Parkinson's disease. *Brain* 132, 1783–1794.
- Orenstein, S.J., et al., 2013. Interplay of LRRK2 with chaperone-mediated autophagy. *Nat. Neurosci.* 16, 394–406.
- Paisan-Ruiz, C., et al., 2005. LRRK2 gene in Parkinson disease: mutation analysis and case control association study. *Neurology* 65, 696–700.
- Park, J.S., et al., 2011. Pathogenic effects of novel mutations in the P-type ATPase ATP13A2 (PARK9) causing Kufor-Rakeb syndrome, a form of early-onset parkinsonism. *Hum. Mutat.* 32, 956–964.
- Plowey, E.D., et al., 2008. Role of autophagy in G2019S-LRRK2-associated neurite shortening in differentiated SH-SY5Y cells. *J. Neurochem.* 105, 1048–1056.
- Poehler, A.M., et al., 2014. Autophagy modulates SNCA/alpha-synuclein release, thereby generating a hostile microenvironment. *Autophagy* 10, 2171–2192.
- Rideout, H.J., et al., 2004. Involvement of macroautophagy in the dissolution of neuronal inclusions. *Int. J. Biochem. Cell Biol.* 36, 2551–2562.
- Ross, O.A., et al., 2008. Genomic investigation of alpha-synuclein multiplication and parkinsonism. *Ann. Neurol.* 63, 743–750.
- Sancho, R.M., et al., 2009. Mutations in the LRRK2 Roc-COR tandem domain link Parkinson's disease to Wnt signalling pathways. *Hum. Mol. Genet.* 18, 3955–3968.
- Schapansky, J., et al., 2014. Membrane recruitment of endogenous LRRK2 precedes its potent regulation of autophagy. *Hum. Mol. Genet.* 23, 4201–4214.
- Sidransky, E., Lopez, G., 2012. The link between the GBA gene and parkinsonism. *Lancet Neurol.* 11, 986–998.
- Su, Y.-C., Qi, X., 2013. Inhibition of excessive mitochondrial fission reduced aberrant autophagy and neuronal damage caused by LRRK2 G2019S mutation. *Hum. Mol. Genet.* 22 (22), 4545–4561.
- Tong, Y., et al., 2010. Loss of leucine-rich repeat kinase 2 causes impairment of protein degradation pathways, accumulation of alpha-synuclein, and apoptotic cell death in aged mice. *Proc. Natl. Acad. Sci. U. S. A.* 107, 9879–9884.
- Trinh, J., et al., 2014. Disease penetrance of late-onset parkinsonism: a meta-analysis. *JAMA Neurol.* 71, 1535–1539.
- Turk, B., et al., 1995. Regulation of the activity of lysosomal cysteine proteinases by pH-induced inactivation and/or endogenous protein inhibitors, cystatins. *Biol. Chem. Hoppe Seyler* 376, 225–230.
- Vilarino-Guelli, C., et al., 2011. VPS35 mutations in Parkinson disease. *Am. J. Hum. Genet.* 89, 162–167.
- Vogiatzi, T., et al., 2008. Wild type alpha-synuclein is degraded by chaperone-mediated autophagy and macroautophagy in neuronal cells. *J. Biol. Chem.* 283, 23542–23556.
- Volpicelli-Daley, L.A., et al., 2016. G2019S-LRRK2 expression augments alpha-synuclein sequestration into inclusions in neurons. *J. Neurosci.* 36, 7415–7427.
- Wang, X., et al., 2012. LRRK2 regulates mitochondrial dynamics and function through direct interaction with DLP1. *Hum. Mol. Genet.* 21, 1931–1944.
- Webb, J.L., et al., 2003. Alpha-synuclein is degraded by both autophagy and the proteasome. *J. Biol. Chem.* 278, 25009–25013.
- West, A.B., et al., 2005. Parkinson's disease-associated mutations in leucine-rich repeat kinase 2 augment kinase activity. *Proc. Natl. Acad. Sci. U. S. A.* 102, 16842–16847.
- Yue, M., et al., 2015. Progressive dopaminergic alterations and mitochondrial abnormalities in LRRK2 G2019S knock-in mice. *Neurobiol. Dis.* 78, 172–195.
- Zimprich, A., et al., 2004. Mutations in LRRK2 cause autosomal-dominant parkinsonism with pleomorphic pathology. *Neuron* 44, 601–607.
- Zimprich, A., et al., 2011. A mutation in VPS35, encoding a subunit of the retromer complex, causes late-onset Parkinson disease. *Am. J. Hum. Genet.* 89, 168–175.